Brain Stimulation 18 (2025) 780–793

Contents lists available at ScienceDirect

Brain Stimulation

journal homepage: www.journals.elsevier.com/brain-stimulation

Predictive role of endogenous phase lags between target brain regions in dual-site transcranial alternating current stimulation

Osama Elyamany [a,b,*], Jona Iffland [a], Josef Bak [a], Cornelius Classen [a], Guido Nolte [c], Till R. Schneider [c], Gregor Leicht [d], Christoph Mulert [a,b]

[a] Centre of Psychiatry, Justus-Liebig University, Klinikstrasse 36, Giessen, Hessen, 35392, Germany
[b] Centre for Mind, Brain and Behaviour (CMBB), Hans-Meerwein-Strasse 6, Marburg, 35043, Hessen, Germany
[c] Department of Neurophysiology and Pathophysiology, University Medical Centre Hamburg-Eppendorf, Martinistraße 52, Hamburg, 20246, Germany
[d] Department of Psychiatry and Psychotherapy, University Medical Centre Hamburg-Eppendorf, Martinistraße 52, Hamburg, 20246, Germany

ARTICLE INFO

Keywords:
Dichotic listening
Interhemispheric connectivity
Dual-site
Bifocal
tACS
EEG

ABSTRACT

Background: Dual-site transcranial alternating current stimulation (tACS) provides a promising tool for modulating interregional brain connectivity by entraining neural oscillations. However, prior studies have reported inconsistent effects on connectivity and behavioral outcomes. They often focused on individualized stimulation-frequency as a key entrainment factor, while typically not focusing on the role of endogenous phase lags. To address this gap, we explored the predictive value of endogenous phase lags in dual-site tACS to modulate interhemispheric connectivity during dichotic listening.

Methods: Thirty healthy participants (16 females) completed a dichotic listening task while undergoing simultaneous electroencephalography and tACS, including four bitemporal verum conditions with varying phase lags (0°, 45°, 90°, and 180°), and a sham condition across five sessions. Each session involved 20 min of 40-Hz tACS at a 0.5 mA peak-to-baseline amplitude applied to the temporal regions, with phase lags differing across sessions. Endogenous phase lags between the auditory cortices were calculated to explain changes in the laterality index (LI) across stimulation conditions by defining optimal and disruptive stimulation conditions for each participant.

Results: Consistent with our hypothesis, our personalized analysis based on the calculated endogenous phase lags showed a significantly lower LI during the closest (optimal) stimulation condition compared to both the sham and farthest (disruptive) conditions. Conversely, the farthest stimulation condition did not statistically increase the LI compared to sham.

Conclusions: These findings highlight the importance of incorporating endogenous phase dynamics into dual-site tACS protocols, paving the way for more consistent and individualized neuromodulatory interventions.

1. Introduction

Transcranial alternating current stimulation (tACS) is a non-invasive brain stimulation (NIBS) technique that delivers sinusoidal alternating electric currents through the skull to modulate activity in targeted brain regions. This approach induces entrainment of endogenous brain oscillations, aligning them with the oscillatory pattern of the external current in a frequency- and phase-dependent manner [1–9]. As a sub-threshold stimulation, tACS does not directly elicit action potentials; rather, it alters the likelihood of neuronal firing within the stimulated regions [10–12]. Simultaneous stimulation of different brain areas by bifocal or dual-site tACS can facilitate the synchronization or desynchronization of their electrical activity and thus enhance or reduce their functional connectivity, respectively. [13,14]. Moreover, tACS has been utilized to modulate EEG-based interhemispheric connectivity metrics such as interhemispheric coherence within the gamma frequency range when applied bilaterally [15,16]. The application of dual-site tACS in various contexts has produced complex and heterogeneous outcomes, particularly concerning the phase lags that can effectively couple or decouple target brain regions. Some previous trials applied dual-site tACS producing different electric field distributions between in-phase and anti-phase conditions [16–21], making it difficult to attribute behavioral outcomes solely to the phase lag without considering these field differences [22,23]. The other studies applying consistent electric fields have

* Corresponding author. Centre of Psychiatry, Justus-Liebig University, Klinikstrasse 36, Giessen, 35392, Hessen, Germany.
E-mail address: osama.elyamany@psychiat.med.uni-giessen.de (O. Elyamany).

https://doi.org/10.1016/j.brs.2025.04.011
Received 18 November 2024; Received in revised form 9 April 2025; Accepted 10 April 2025
Available online 11 April 2025

observed behavioral and connectivity changes with in-phase [13,14,24–29], or with anti-phase tACS [14,28–30], while others did not report any effects at all [31,32]. Therefore, focusing exclusively on stimulation phase lags, while ignoring the endogenous brain state, may not be sufficient to predict tACS outcomes, especially since its effects have been shown to depend on the internal brain states, including individual endogenous phase lags, cross-frequency coupling, inherent wave propagation speeds, and the level of cognitive demands [17,18,26,30,32,33]. Consequently, it may be important to investigate the interaction between the endogenous interhemispheric phase lags and the externally applied phase lags to predict the resulting behavioral changes under tACS, rather than focusing solely on the external phase lags introduced by the stimulation.

The dichotic listening (DL) task simultaneously presents two different sounds one to each ear, where participants report the perceived sound (illustrated in Fig. 1). Typically, individuals with left-hemispheric dominance report more sounds from the right ear, a phenomenon known as the "right ear advantage" (REA) [34–36], first described by Kimura in 1961 [37,38]. This occurs because contralateral processing of auditory stimuli is the predominant pathway during dichotic listening, which includes the inhibition of ipsilateral processing [39]. Accordingly, sounds heard in the right ear directly access the left (dominant) hemisphere. In contrast, sounds from the left ear first reach the right hemisphere and then have to pass the corpus callosum to be processed in the left hemisphere requiring stronger interhemispheric connectivity between the auditory cortices [40,41]. The REA is also influenced by reciprocal inhibition between the auditory cortices during DL [42]. This concept, known as the "callosal relay model" [40], is demonstrated in Fig. 1. Using electroencephalography (EEG), previous studies have addressed the interhemispheric connectivity between auditory cortices during DL [43–51]. The results indicate that left ear reports are correlated with enhanced interhemispheric communication in the gamma frequency range [48,51], supporting the callosal relay model (Hugdahl and Westerhausen, 2016). Furthermore, the information flow was reported to be stronger in the right-to-left direction during left-ear reports [49]. These findings are corroborated by diffusion tensor imaging, which reveals anatomically stronger interhemispheric communication in association with enhanced interhemispheric communication [46].

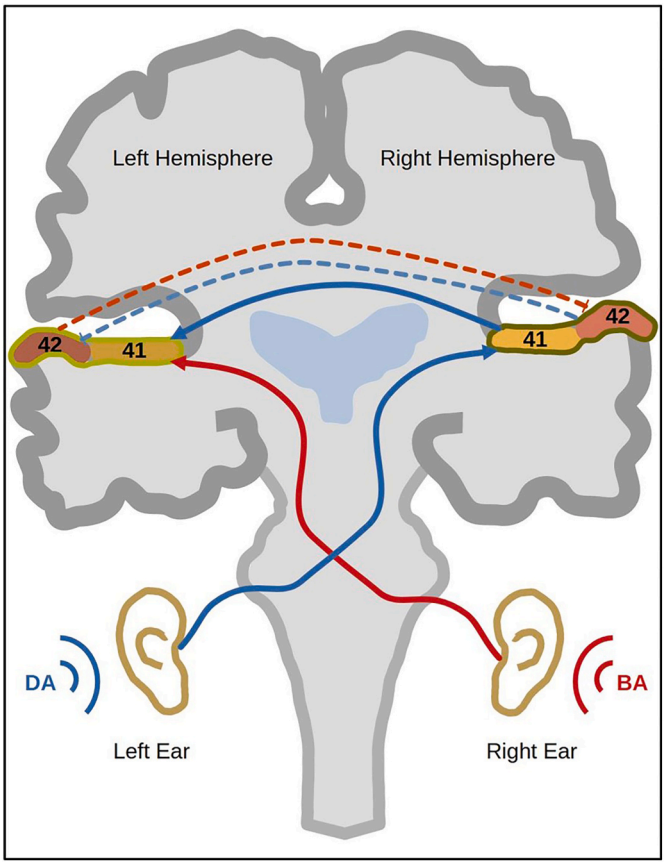

Fig. 1. Schematic representation of dichotic listening and its corresponding auditory pathways. This illustration depicts a dichotic listening trial where the sound "BA" is delivered to the right ear and "DA" to the left ear. It also illustrates how auditory information is processed, where the sound from the right ear is directly routed to the left auditory cortex, which is the dominant hemisphere. Conversely, the sound from the left ear first reaches the right auditory cortex before crossing the corpus callosum to the left hemisphere. This processing route explains why the majority of participants exhibit a right ear advantage (REA). The dashed lines represent the reciprocal inhibition between the auditory cortices during dichotic listening.

Four previous publications have explored the use of simultaneous bitemporal tACS to modulate interhemispheric connectivity during DL, thereby influencing auditory perception at the behavioral level [29,32,52,53]. Upon applying anti-phase (180°-phase lag) of gamma (40 Hz) tACS, our research group did not observe differences in REA compared with sham stimulation. However, the post-hoc analysis demonstrated that the endogenous phase asymmetries could help predict the directionality of REA changes during the stimulation at the individual level [32]. Another study stimulated bitemporal regions with two frequencies: gamma (40 Hz) and delta (3.125 Hz), each was applied with two-phase conditions: in-phase (0°-phase lag) and anti-phase (180°-phase lag compared to sham stimulation, both in-phase gamma and anti-phase delta tACS disrupted the interhemispheric integration of dichotically presented auditory stimuli [29]. To investigate the interhemispheric connectivity, the same research group applied gamma (40 Hz) tACS with the same two-phase conditions while measuring the effective brain connectivity via functional magnetic resonance imaging (fMRI). Contrary to the previous study, neither stimulation condition showed behavioral differences, although anti-phase gamma tACS reduced interhemispheric connectivity, which correlated with a reduction in binaural integration at the behavioral level [52]. Upon individually simulating the electric field strength, the tACS effects on interhemispheric connectivity could be predicted by the right hemispheric electric field strength. However, it could not predict the behavioral interhemispheric integration [53]. This adds further complexity to the role of interhemispheric communication during DL, highlighting the need for more in-depth research into the underlying endogenous phase lags and their interactions with tACS effects.

In the current study, we aimed to investigate how the endogenous phase lags between the auditory cortices could predict the effects of bilaterally applied tACS during DL. Building on our previous research, we applied tACS with four different phase lag conditions between the temporal stimulation sites and compared these effects to a sham condition [32]. Based on our previous findings, we hypothesized that the synchronization and desynchronization of the auditory cortices under different tACS phase lags would depend on the interaction between endogenous phase lags and the stimulation conditions, rather than on the stimulation conditions per se.

2. Methods

Healthy participants were recruited for five sessions, each spaced one week apart, after signing an informed consent according to the approval of the ethical committee at the Faculty of Medicine (FB 11 Medizin), Justus-Liebig University Giessen, registered with the project number "AZ 34/19". During each session, the participants performed a DL task under simultaneous tACS and EEG recording (Fig. 2 Panel (C)). We included right-handed individuals of any gender aged between 18 and 65.

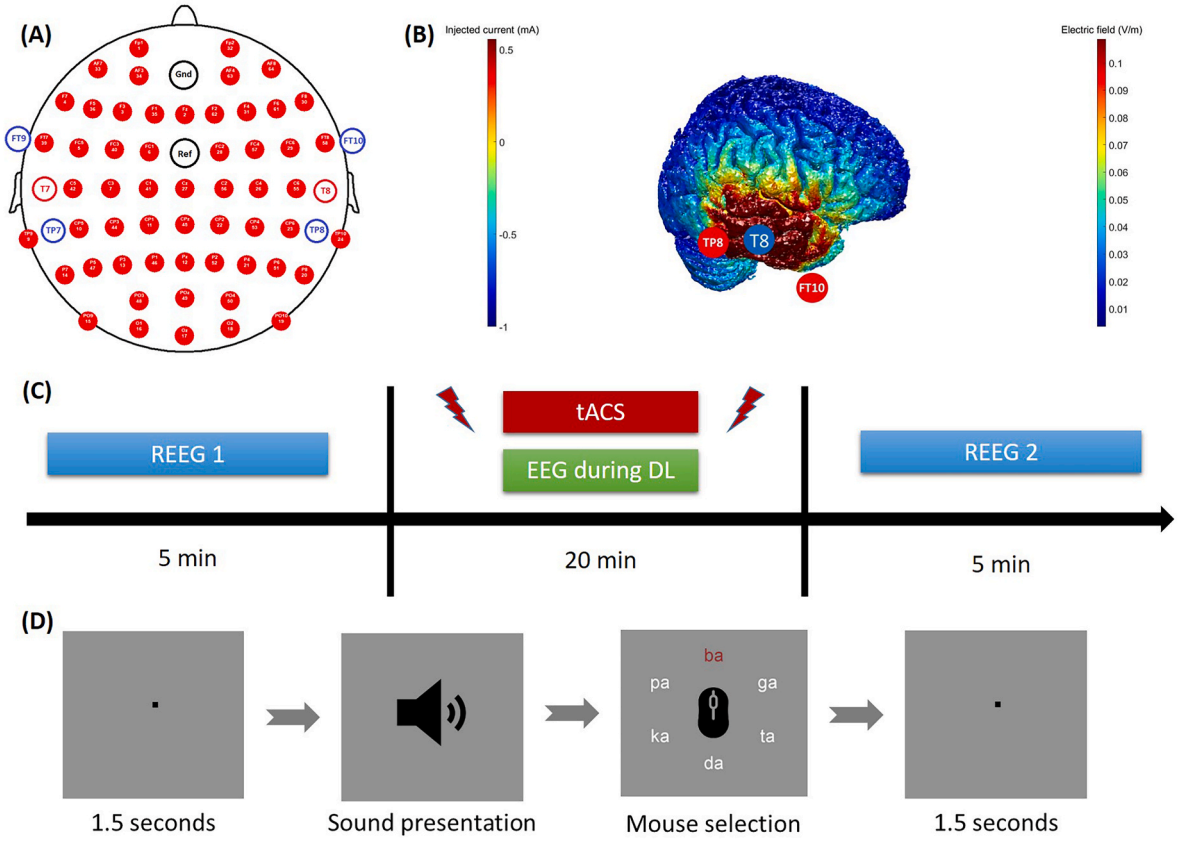

Fig. 2. Methodological setup of the main experiment. Panel (A) shows our EEG-tACS electrode configuration, where we used an extended version of the 10/20 system with 64 electrode positions. The reference and ground electrodes were placed at FCz and AFz, respectively, while electrooculography (EOG) was measured by four electrodes: superior and inferior vertical electrodes (VEOGS and VEOGI) and right and left horizontal electrodes (HEOGR and HEOGL). The stimulation was applied bilaterally and simultaneously at the temporal regions. Panel (B) shows the simulation of the injected current and the resulting electric field via the ROAST toolbox. It demonstrates the electric filed distribution on the right temporal side upon applying external electric current with an amplitude of 278 μA and 222 μA at FT10 and TP8 respectively, while the T8, as the central electrode, received a current of 0.5 mA peak-to-baseline (i.e., 1 mA peak-to-trough). As depicted, this stimulation protocol perfectly targets Brodmann area 42 (the second auditory cortex), located on the superior temporal gyrus. The left side had the same configuration using the corresponding electrodes (central: T7, stimulating: FT10 and TP8). Panel (C) shows the study design for each stimulation session, which started and ended with a resting EEG (REEG) for 5 min. Between both REEGs, the dichotic listening (DL) task was run during simultaneous tACS and EEG recording for 20 min. Panel (D) shows one of the dichotic listening trials used during the experiment. The trials started with a fixation point for 1.5 s and then the sound was presented. Afterwards, the participant had to select - with the left button of the mouse using the right hand - the best-heard syllable out of six different options (ba - da - ga - pa - ta - ka). After confirmation of the selection with a right click, the next interval of 1.5 s was activated.

2.1. Participants

The criteria for inclusion encompassed individuals of any gender within the age range of 18–65, who were right-handed and spoke German as their native language. Exclusion criteria consisted of left-handedness, hearing impairment, presence of any neurological or psychiatric conditions, tACS contraindications (biomedical implantations, epilepsy, heart disease, etc.), or the use of medications known to impact brain function.

2.2. Questionnaires

Before the first session, the participants had to fill in a questionnaire for sociodemographic data, the Schizotypal Personality Questionnaire (SPQ) [54] and the Edinburgh Handedness Inventory (EHI) [55]. The SPQ helped to exclude the participants with high schizotypal personality traits, who might show abnormally reduced right ear advantage [56]. Before each stimulation session, two other questionnaires were used: one to screen for the contraindications of tACS and another to collect information about the various factors that could affect the tACS response, such as medication use, caffeine consumption, smoking, alcohol intake, and sleep patterns. The later questionnaire allowed to further assess the inclusion/exclusion criteria. After each stimulation, a questionnaire for the expected side events of tACS was completed with the help of the experimenter. The last three mentioned questionnaires were developed according to the previously recommended guidelines of transcranial electric stimulation [57–59]. Since we applied the stimulation in a single-blinded manner, the participants had to report after each session if they received a sham or a verum stimulation, to assess for the blinding.

2.3. Audiometry

Before running the DL task in each session, audiometry was carried out using the Home Audiometer Hearing Test [60]. The participants were tested with three sound frequencies (500 Hz, 1000 Hz and 2000 Hz). The inclusion criterion was the hearing ability of sounds below 15 dB for each ear with an interaural difference below 9 dB.

2.4. Dichotic listening

We used the Bergen CV paradigm and setup, described in our previous publication [51]. The participants were presented with voiced and unvoiced pairs made of six syllables (ba-da-ga-pa-ta-ka), pronounced by

a male native German speaker. The syllable durations had a mean of 0.3674 s and a standard deviation of 0.0256 s. To minimize any potential bias from differences in syllable duration, we paired only homologous syllables (voiced-voiced and unvoiced-unvoiced) [61]. Specifically, we selected the following 12 pairs: voiced pairs (ba-ga, ba-da, da-ba, da-ga, ga-da, and ga-ba) and unvoiced pairs (pa-ka, pa-ta, ta-pa, ta-ka, ka-ta, and ka-pa). The paradigm consisted of two separate blocks, each comprising 120 trials (240 trials in total). The trials were run using Presentation® software [62] and began with the display of a fixation point for 1.5 s, followed by the auditory presentation of the syllables. Participants were then required to select the syllable they perceived most clearly from six options (ba, da, ga, pa, ta, ka) via clicking the left mouse button using the right hand. After confirming their choice with a right click, the next trial began following a 1.5-s interval (Fig. 2 Panel (D)). The left and right ear reports (LE or RE) for each session/participant were analyzed to calculate a laterality index (LI), as a measure of REA using the following formula:

$$LI = (RE - LE) \,/\, (RE + LE) \times 100$$

2.5. tACS

We applied five different stimulation protocols in a single-blinded fashion: one sham stimulation and four different verum stimulations. Each verum stimulation included 20-min tACS at the frequency of 40 Hz with a peak-to-baseline amplitude of 0.5 mA. The stimulation was applied simultaneously bilaterally to the left and the right temporal areas, notably targeting the secondary auditory cortices, Brodmann Areas (BAs) 42. To achieve this, high-definition tACS was delivered using the DC-Stimulator MC (NeuroConn) [63], which provides four possible pairs of channels with opposing polarities. Additionally, the stimulation parameters such as current intensity and phase at current onset for each pair can be set independently. Both EEG and tACS electrodes were positioned according to the extended 10–20 system. For each hemisphere, the current was delivered via two scalp electrodes connected to two channels of the stimulator, with the two opposing channels connected to a single central electrode. Over the left hemisphere, two electrodes of the same polarity were placed at FT9 and TP7 and the electrode with the opposing polarity at T7. Analogously, over the right hemisphere two electrodes were positioned at FT10 and TP8 and the electrode with opposing polarity at T8. In total, all four pairs of channels of the stimulator were used. The alternating current was injected through the electrodes on the left side with the following amplitudes: 278 μA at FT9 and 222 μA at TP7, which sum up to 500 μA peak-to-baseline (i.e., 1 mA peak-to-trough) at the central electrode T7. By analogy, the same currents were injected on the right side at FT10 (278 μA) and TP8 (222 μA) summing up to 500 μA at the central electrode T8 with opposing polarity.

To ensure stimulating the target regions (left and right BAs 42), the electrode positioning and their current intensities were simulated using the ROAST toolbox [64]. The electric field simulation showed the targeting of the regions of interest, i.e., left and right BAs 42 located on the superior temporal cortex (Fig. 2 Panel (B)) [65,66]. We used six Ag/AgCl electrodes (12 mm diameter) [67], and their contact points were cleaned with alcohol to remove skin secretions. An electro-conductive gel (Signagel® Electrode Gel) was applied to maintain skin-electrode resistance below 5 kΩ [68].

The sham stimulation consisted of two phases: a 10-s ramping-up to the maximum current intensity followed by a 30-s ramping-down. For the verum stimulation, the same durations of ramping-up and ramping-down were set, but the stimulation lasted for 20 min in between. The four stimulation conditions had exactly the same parameters except for the phase difference between the left and right stimulation sites. Phase lags of 0°, 45°, 90°, and 180° were applied, with the alternating current on the right hemisphere leading the left to achieve these differences, by modulating the onset phase of the right-sided current. Each participant received all five stimulation conditions (one per session) in a randomized sequence, while the order of the sessions was counterbalanced across the participants.

2.6. EEG recording

EEG was recorded using a 64-channel EEG system, composed of two (BrainAmp DC) amplifiers, each connected to 32 passive electrodes [69] (Fig. 2 Panel (A)). To maintain the electrical resistance below 5 kΩ, an electro-conductive gel connected the electrodes to the skin surface [70]. The recording was controlled by Brain Vision Recorder software version 1.21.0303 at a sampling rate of 5000 Hz [71]. Each session consisted of the same sequence of EEG recordings: a 1st resting EEG recording, followed by a simultaneous tACS-EEG recording (while performing the DL paradigm), and finally a 2nd resting EEG recording (Fig. 2 Panel (C)). The datasets form the resting EEGs were not considered within the scope of this paper.

2.7. EEG pre-processing

Since there is no consensus in the literature for the correction of tACS-induced EEG artefacts, we focused our EEG analysis on the EEG recordings of the DL task during the artefact-free sham stimulation, similar to our previous study [32]. Resting EEGs were not analyzed within the scope of this current paper. For pre-processing, we used Brain Vision Analyzer software version 2.2 [72]. We started by creating a radial EOG channel to correct the micro-saccadic artefacts later using ICA applying the following formula [73]:

$$\mathrm{REOG} = \{(\mathrm{VEOGS} + \mathrm{VEOGI} + \mathit{HEOGR} + \mathrm{HEOGL}) \;/\; 4)\} - \mathrm{Pz}$$

Since these artefacts are confined to the gamma band, the newly created channel was subjected to a filter from 30 to 100 Hz. Other channels were filtered from 1 to 100 Hz to improve the results of independent component analysis (ICA) [74]. All Filters were linear (zero-phase) non-causal finite impulse response (FIR) filters using the default filtering tool of EEGLAB [75] as a recommendation from the previous literature [76]. Also as recommended, the high-pass and the low-pass filters were run separately to apply the corresponding default filter orders. To correct the channel noise, the CleanLine EEGLAB plugin was run at the frequency of 50 Hz with default parameters on all datasets after filtering [77]. Afterwards, the datasets were down-sampled to 250 Hz. In a semiautomatic way, the resulting EEGs were inspected to remove any epochs containing non-repeating artefacts or non-correctable channels. Then, all channels were re-referenced to a common average reference while retaining FCz as a separate channel. The resulting EEG and EOG channels were subjected to an extended infomax ICA with 512 iterations to decompose 60 components (since the data rank was 60, while the number of channels was 61). The components were then inspected according to their time series, topography, frequency composition and stacked plots to remove the corresponding artefacts (eye: vertical, horizontal and micro-saccadic movements; heartbeats; muscle; and artificial: line noise, channel noise and stimulator-related artefacts). Afterwards, the four EOG electrodes were deleted, keeping 57 EEG channels. To investigate the endogenous gamma activity at 40 Hz, the cleaned datasets were re-filtered from 39 to 41 Hz using the same filter settings, as we stimulated at 40 Hz. The datasets were then segmented from – 200 ms to 824 ms around the presented stimulus (the played sound pair) into two different conditions: LE and RE. Finally, they were baseline-corrected to be forwarded to the phase lag analysis.

2.8. Phase lag analysis

Similar to our previous analysis, we extracted the endogenous phase lag between auditory cortices from the EEG recordings of the DL task during the artefact-free sham condition via exact low-resolution brain

electromagnetic tomography (eLORETA) [32,78–80]. eLORETA utilizes a three-shell spherical head model and employs the MNI (Montreal Neurological Institute) brain template for source localization, based on the Talairach atlas. We used the remaining 57 electrodes with their default manufacturer coordinates to build the transformation matrix using the eLORETA algorithm. Within the resulting transformation matrix, we defined our regions of interest (ROIs) as a centroid voxel with a spatial resolution of 5x5x5 mm^3 within Brodmann Areas (BAs) 42 [81]. These areas represent the secondary auditory cortex, a key integration region for auditory interhemispheric communication, based on our previous results [32,46,48,49,51]. The pre-processed peri-stimulus segments (i.e., from – 200 ms to 824 ms around the presented stimulus) were inserted into the connectivity analysis of eLORETA to extract the time series of XYZ components of the current density within the ROIs. Since the sample size of the EEG segments could cause a bias in the calculation of the phase lags, we matched the numbers of the segments for each participant. The number of corresponding segments (LE vs RE) was matched to the minimum number of both conditions for each participant using Python [82]. On average, the matched number of segments per participant was 70.7, with a standard deviation of 25.1, ranging from 26 to 113 segments. Further analysis was accomplished using MATLAB scripts [83]. To calculate the phase lags $\Delta\varphi$ for each time point (t) between right and left ROIs, we computed the angle of the multiplication product resulting from multiplying the Hilbert-transformed right-sided component by the complex conjugate product of the Hilbert-transformed left-sided component, using the following formula:

$$\Delta\varphi(t) = angle\left[\, hilbert\left(\, X_{right}(t)\,\right) \times conjugate\left(\, hilbert\left(\, X_{left}(t)\,\right)\right)\,\right]$$

In this computation, the Hilbert transform (hilbert () function) was used to obtain the analytic signal, which provides a complex representation of the original signal, with the real part being the original signal and the imaginary part being the Hilbert transform of the signal [84–87]. The complex conjugate of the Hilbert-transformed second signal was computed using the conj() function, which was necessary for the subsequent computation of the phase difference. The multiplication combines the phase information of the two signals, where the angle() function was then used to extract the phase angle of the resulting complex signal for each time point. This phase angle represented the phase difference between the two original signals from both ROIs, where the right side always preceded the left side (according to our phase lag calculation formula), since we were interested in the right-to-left connection. A positive angle indicates that the right side was preceding the left by less than half a cycle, while a negative angle indicates it was by more than half a cycle. Further analysis of the angular data was assisted by the CircStat toolbox from MATLAB [88]. To obtain a single representative phase lag value in the form of a time series, we averaged the phase lags across trials and then across the dimensional components for each participant at each time point using the circ_mean() function. At this stage, we could get individual time series for the phase lags between BAs 42 during two different conditions (LE vs RE). These time series (−200 to 824 ms after the stimulus presentation with a sampling rate of 250 Hz) were subjected to further statistical analysis to extract a relevant time window, where LE could show statistically different phase lags in comparison with RE. This specific time window would represent the determinant time interval, at which the phase lag between BAs 42 plays a key role in interhemispheric signal communication during LE [32].

To extract this critical time window, we applied three restrictive criteria to minimize the effects of random noise and multiple comparisons. First, the differences between LE and RE at the time points of this time window should withstand a non-parametric paired-sample permutation test suitable for circular data (see statistical analysis) i.e., show statistically significant differences between LE and RE. Second, this time window should comprise a meaningful cluster of consecutive time points that are not arbitrarily significant. Since we were interested in the signal of 40 Hz with a sampling rate of 250 Hz, a meaningful cluster of time points should cover at least the length of one 40-Hz wavelet, i.e., 25 ms ≈ 6 time points. Third, the determinant time window should overlap with reliable and reproducible time windows, extracted from a test-retest reliability experiment for a similar DL task. Once extracted, we could average the individual phase lags across this time window during LE via the circ_mean() function. These individually averaged phase lags could then be correlated circularly with the behavioral parameters during each stimulation condition using the CircStat toolbox. This helps discover any circular dependencies between the endogenous phase lags and the LIs of the different stimulation conditions.

Afterwards, we adopted a personalized analytical approach to explain the heterogeneity of behavioral DL changes across the four different stimulation conditions. Based on the resulting individual determinant phase lags during LE, we could define which of our four stimulation conditions would be optimal or detrimental for the interhemispheric communication within each participant. For example, a participant with a phase lag of 50° would theoretically benefit most from the stimulation condition with the 45°phase lag (closest stimulation condition), while their interhemispheric synchronization would be most disrupted during the stimulation condition with the 180° phase lag (farthest stimulation condition). Therefore, we hypothesized that the closest and the farthest stimulation conditions for each participant would, in turn, increase and decrease the reports from the left ear, and thus reduce and enhance the REA, respectively. Considering the natural physiological requirement for a non-zero phase lag in interhemispheric connectivity, we excluded the 0° phase lag condition from the analysis of determining the closest stimulation condition [85,89]. This exclusion allowed for a more accurate comparison of the closest and farthest conditions, along with the sham condition, in terms of the LI. This personalized approach provided a nuanced understanding of how each stimulation condition impacted interhemispheric communication and DL performance at the individual level.

2.9. Test-retest reliability

In order to test the reliability of the behavioral (LIs) and the neurophysiological (internal phase lags) parameters, we conducted a test-retest version of (dichotic listening) DL. Therefore, we recruited healthy male participants for two sessions (two week apart) to perform a similar DL task with simultaneous Electroencephalography (EEG) recording without transcranial alternating current stimulation (tACS). The recruitment was restricted to males only to avoid any gamma band changes induced by the different menstruation phases [90,91]. The other inclusion/exclusion criteria were the same as those of the main experiment. To obtain more reliable results, the participants performed a DL task with three blocks instead of two. To optimize the EEG signal, we utilized active EEG electrodes [92]. The other settings for recording and analysis of EEG data were similar to those above-mentioned to extract the determinant time window of interhemispheric connectivity and the internal phase lags, except for the sampling rate, which was higher (500 Hz) for this test-retest reliability to get better temporal resolution. Therefore, the minimum of significant time points was set at 12 consecutive time points that should be reproducible in both sessions.

2.10. Statistical analysis

The continuous data was summarized with the mean ± standard deviation (SD), while the categorical data was expressed with numbers and percentages. Figures illustrating comparisons presented means along with 95 % confidence intervals, whereas the time series of phase lags were depicted with thick lines representing the circular means (using the circ_mean() function) and shaded areas indicating circular standard deviations (via the circ_std() function). The time series of phase lags were generated using MATLAB software [83]. For inferential statistics, we chose the suitable test according to the nature of the data.

First, the LIs from the five stimulation conditions were compared using a one-way repeated-measures analysis of variance (ANOVA) with Greenhouse-Geisser correction since Mauchly's sphericity test showed significance. Second, a non-parametric paired-sample permutation test suitable for circular data was used to detect the determinant time window, where LE showed statistically different phase lags compared with RE [93,94]. The test corrects inherently for multiple comparisons after 10000 permutations independent from the data distribution. Third, to examine the circular correlations between the endogenous phase lags at the determinant time window and the behavioral parameters (LIs), we utilized the circ_corrcl() function from the CircStat toolbox. Fourth, a one-way repeated-measures ANOVA was applied to compare the LIs between the closest, farthest, and sham stimulation conditions with correction as Mauchly's sphericity test was not significant. Then, post-hoc three one-sided paired-sample t-tests were conducted for pairwise comparisons, anticipating the LI to behave in a specific direction. Specifically, the closest stimulation condition was expected to show a reduced LI compared to the other two conditions, while the farthest stimulation condition was expected to increase the LI relative to the sham condition. To account for multiple comparisons, the resulting p-values were adjusted using the Benjamini-Hochberg (BH) method to control the false discovery rate [95]. Both JASP [96] and SPSS [97] software packages were employed for the analysis. Statistical significance was defined as a p-value below 0.05. The complete statistical analysis is detailed in Supplementary Material S1.

3. Results

3.1. The inclusion/exclusion criteria yielded thirty eligible participants

We recruited 32 participants (17 females), but two participants were later excluded: one male for being left-handed and one female for missing a stimulation session due to the development of a psychiatric disorder. The remaining 30 participants (16 females), aged between 19 and 58 years (mean age: 27.4 ± 9.15 years), were all right-handed according to the EHI. They participated in all five stimulation sessions, with an average intersession interval of 8.84 ± 4.48 days. None of the participants exhibited identifiable schizotypal personality traits based on the SPQ. All participants had normal hearing, with the ability to perceive sounds below 15 dB and an interaural difference of less than 9 dB.

3.2. The tACS conditions were tolerated and successfully applied in a single-blinded manner

No serious adverse events were reported by the participants. However, some participants experienced minor local skin sensations, including irritation, burning, and warmth. Regarding blinding, participants were asked to identify whether they received verum tACS (irrespective of the specific phase lag) or sham stimulation. They correctly identified the stimulation condition in 84 out of 150 sessions, resulting in a correct identification rate of 56 %.

3.3. The stimulation conditions did not significantly change laterality index compared with sham

Responses for each session from all 30 participants were correct (reporting the syllable presented to either the left or right ear) in more than 75 % of the 240 trials (mean = 225.12 ± 12.36), so all participants were included in the behavioral analysis. During the sham stimulation condition, 29 participants (97 %) exhibited a positive laterality index (LI), indicating a REA, while only one participant showed a left-ear advantage (LI = −0.44). The sham condition exhibited an LI of 37.3 ± 24.1, with a range from −0.44 to 78.8. In comparison, the stimulation conditions yielded the following LIs: 0° = 36.3 ± 23.7, 45° = 35.2 ± 21.4, 90° = 34.9 ± 26.1, and 180° = 35.0 ± 23.1.

A one-way repeated-measures ANOVA on the LIs from all stimulation conditions revealed no significant effect of tACS condition ($df = 2.58$, $F = 0.350$, $p = 0.759$, $\eta^2p = 0.012$). The Greenhouse-Geisser correction was applied due to the significant result of Mauchly's test of sphericity ($P < 0.001$) (Fig. 3).

3.4. The endogenous phase lags could predict the changes in LIs

The time series of the endogenous phase lags are shown in Fig. 4 Panel (A), where the right side was the leading side, according to our phase difference calculation formula. A non-parametric paired-sample permutation test with 10,000 permutations revealed that the LE showed significantly different phase lags compared to the RE in the time window between time points 71 and 78, which corresponds to 84–112 ms after stimulus presentation (p-values = 0.0057, 0.0311, 0.005, 0.0326, 0.0467, 0.0133, 0.0211). This time window met our second criterion of covering seven consecutive time points and also met the third criterion as it overlapped with a reproducible significant time window from test-retest reliability.

On average, left ear reports exhibited positive phase lags, indicating a relatively small phase lag, compared to the negative phase lag during right ear reports. This finding was replicated in both sessions of test-retest reliability. Endogenous phase lags were averaged within these time points during LE for each participant, resulting in the circular distribution shown in Fig. 4 Panel (B) and Table 1. Circular correlations between endogenous phase lags and the differences in LIs between each stimulation condition and the sham condition showed a statistically significant correlation only during the 180° phase lag stimulation condition ($r = 0.48713$, $P = 0.028453$) (Fig. 4 Panel (C)). Results for other correlations are detailed in the Supplementary Material S1.

The closest and farthest stimulation conditions exhibited LIs of 33.1 ± 22.5 and 38.1 ± 22.4, respectively, compared to the sham condition, which had an LI of 37.3 ± 24.1. Using a one-way repeated-measures ANOVA, the comparison of LIs between the closest, sham, and farthest stimulation conditions showed statistical significance ($df = 2$, $F = 3.724$, $p = 0.030$, $\eta^2p = 0.114$).

Applying one-sided paired-sample t-tests, the **post-hoc** pairwise comparisons showed statistically lower LI (indicating lower REA) during the closest stimulation condition compared with the sham condition ($t = -2.031$, $df = 29$, $p = 0.026$, BH-corrected $p = 0.039$) and the farthest stimulation condition ($t = -2.449$, $df = 29$, $p = 0.010$, BH-corrected $p = 0.03$) (Fig. 5). The comparison between the sham and farthest stimulation conditions did not reach statistical significance ($t = -0.440$, $df = 29$, $p = 0.332$, BH-corrected $p = 0.332$).

3.5. Test-retest reliability showed the stability of the behavioral (LIs) and the neurophysiological (internal phase lags) parameters

We recruited 30 healthy male participants, two of them were later excluded since they showed non-right ear advantage according to the EHI [55]. To investigate the test-retest reliability at the behavioral level, we a applied a Pearson's correlation between the laterality indices (LIs) of both sessions, which showed a significant positive correlation ($r = 0.761$, $p = 2.546 \times 10^{-6}$) (Fig. 6).

For the phase lag analysis, we applied the same calculations as these for the main experiment. So, we created a time series of phase lags between the right and left auditory cortices for each session (Fig. 7 Panel (A) & (B)). Afterwards, we applied the same a non-parametric paired-sample permutation test to extract the determinant time window, which shows significant difference in phase lags between the left and the right ear reports (LE Vs RE). In session 1, we found a significant cluster of time points between 150 and 163, which indicates the time window between 100 and 126 ms after the stimulus presentation. In the case of session 2, an overlapping significant time window was obtained between the time points between 151 and 163, i.e., the time window between 102 and 126 ms after the stimulus presentation, except for a near-significance

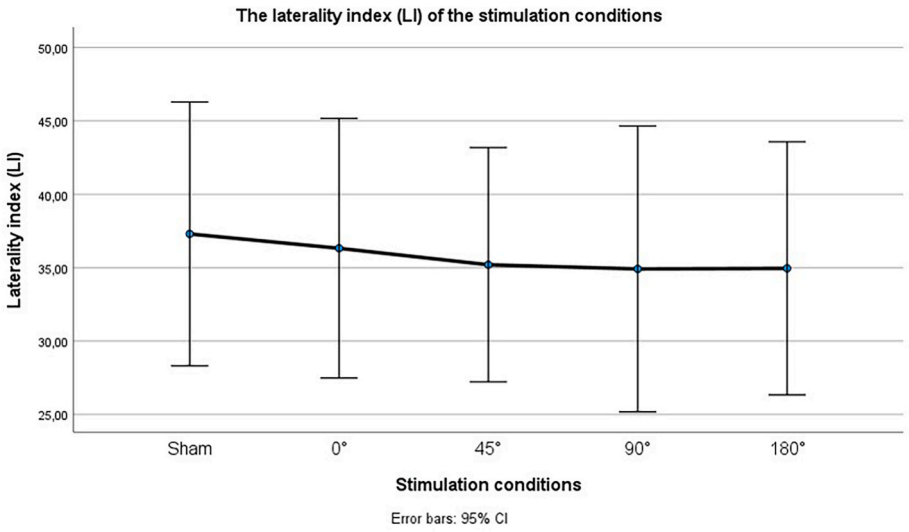

Fig. 3. The stimulation conditions did not significantly change LIs compared with sham. The figure shows the comparison of the five stimulation conditions in terms of the laterality index (LI). The one-way repeated-measures ANOVA indicated no significant differences between the stimulation conditions (df = 2.58, F = 0.350, p = 0.759, η^2p = 0.012). The dots represent the means while the error bars represent the confidence intervals.

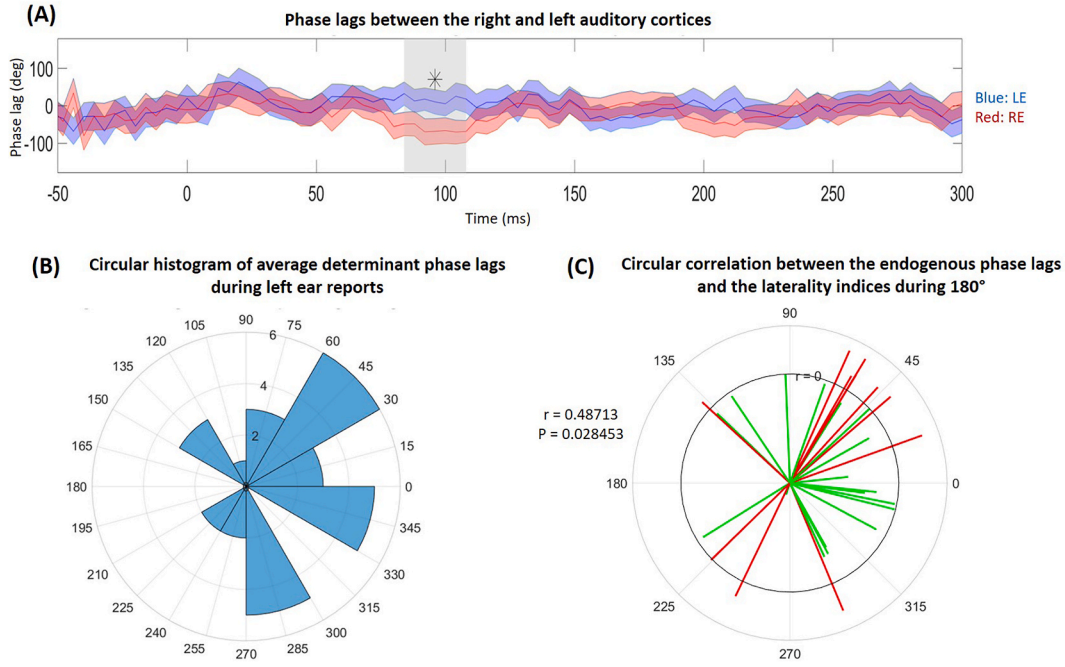

Fig. 4. Extraction of the relevant endogenous phase lags and their distribution. Panel (A) shows the time course of phase lags between the right and left secondary auditory cortices Brodmann areas (BAs) 42, where the right side was the leading side (according to our calculation formula), since we were interested in the interpretation of right-to-left connection. Compared with right ear reports (RE) (in red), the left ear reports (LE) (in blue) exhibited significantly different phase lags in the time window between time points 71 and 78, translating to 84–112 ms after stimulus presentation (p-values = 0.0057, 0.0311, 0.005, 0.0326, 0.0467, 0.0133, 0.0211). Thick red and blue lines represent the means, while shaded areas indicate standard deviations. The grey-shaded area with the asterisk denotes the significant time window. Panel (B) shows a circular histogram for the endogenous phase lags (average within significant time points during LE for each participant), with the radius indicating frequencies in steps of 2:6. Panel (C) presents a significant circular correlation between endogenous phase lags and differences in laterality indices (LIs) between the 180° stimulation and sham conditions (r = 0.48713, P = 0.028453). The circle with radius r = 0 indicates no difference in LI between the two conditions, while line lengths reflect the direction of LI changes (red and green represent changes towards REA and left-ear advantages, respectively). A red line exceeding the zero limit (positive LI difference) indicates a shift towards REA during 180° stimulation compared to sham. Given that many participants exhibited an endogenous phase lag between −45° (315°) and 90° (Panel (B)), a substantial number may have experienced a shift towards REA during 180° tACS (indicating a disruptive tACS effect).

time window 157–158 (p = 0.069). Similar to the main experiment, left ear reports on average exhibited positive phase lags, indicating a relatively small phase lag, compared to the negative phase lag during right ear reports.

Similar to the main experiment, we calculated the average phase lags from the significant time windows during left ear reports (LE) as a representative value for the endogenous phase lags. For this, we selected the overlapping time window between the time points 151 and 163

Table 1
The endogenous phase lags and their corresponding closest and farthest stimulation conditions.

Endogenous Phase Lag in radians	Endogenous Phase Lag in degrees	Closest stimulation condition	Farthest Stimulation condition
0.709105	40.628700	45	180
4.108455 (−1.17473)	292.693200 (−67.306800)	45	90
0.106121	6.080273	45	180
1.611.704	92.343830	90	0
3.698485 (−2.5847)	211.908000 (−148.092000)	180	45
5.213055 (−1.07013)	298.685800 (−61.314200)	45	90
6.179825 (−0.10336)	354.078020 (−5.921980)	45	180
1.004.318	57.543180	45	180
1.024.008	58.671330	45	180
5.226585 (−1.0566)	299.461400 (−60.538600)	45	90
2.379.082	136.311300	180	0
5.150035 (−1.13315)	295.075400 (−64.924600)	45	90
0.346217	19.836770	45	180
239.652	137.310500	180	0
1.049.998	60.160460	45	180
5.791065 (−0.49212)	331.803300 (−28.196700)	45	180
0.828611	47.475900	45	180
5.207705 (−1.07548)	298.379700 (−61.620300)	45	90
1.022.061	58.559800	45	180
4.379845 (−1.90334)	250.947000 (−109.053000)	180	90
6.086195 (−0.19699)	348.713100 (−11.286900)	45	180
4.263395 (−2.01979)	244.275000 (−115.725000)	180	45
2.161.488	123.844200	90	0
3.913835 (−2.36935)	224.246000 (−135.754000)	180	45
6.036885 (−0.2463)	345.888100 (−14.111900)	45	180
1.147.296	65.735210	45	180
6.152235 (−0.13095)	352.496920 (−7.503080)	45	180
1.232.396	70.611080	90	180
0.515718	29.548450	45	180
0.751053	43.032160	45	180

(102–126 ms after the stimulus presentation) as the determinant one, which is longer than 12 consecutive time points (minimum criterion). The endogenous phase lags for each session are presented in Fig. 7 Panel (C) & (D). In order to test for the reliability and stability of these endogenous phase lags, we applied a circular correlation between these circular variables using the function circ_corrcc() provided by the CircStat toolbox. The test resulted in a significant circular correlation between both of them ($r = 0.3917$, $p = 0.0224$).

4. Discussion

4.1. Summary of results of the current study

In the current study, we applied in addition to sham stimulation four different tACS stimulation conditions with four different phase lags (0°, 45°, 90° and 180°) between both stimulation sites (bilateral temporal cortices) in 30 healthy participants, while they performed a DL task during simultaneous EEG recording. We stimulated at the frequency of 40 Hz for 20 min with an amplitude of 0.5 mA peak-to-baseline (i.e., 1 mA peak-to-trough) at each stimulation site. We hypothesized that the tACS effects at the behavioral level would depend on the interaction between the endogenous and the external phase lags. Therefore, we personalized our analysis and defined for each participant the closest and the farthest stimulation conditions based on the endogenous phase lags. In line with our hypothesis, this novel personalized statistical analysis (i.e., comparison of LIs between the closest and sham, and farthest stimulation conditions) showed significantly lower LI (lower REA) during the closest compared with the sham and farthest stimulation conditions. Conversely, the farthest stimulation condition did not lead to a statistically significant increase in the LI compared to the sham condition. To validate our results, we ran a similar test-retest reliability experiment, which revealed the reliability and stability of both behavioral outcomes (LIs) and endogenous phase lags in terms of their determinant time window and their individual values. On the other hand, based on the stimulation conditions alone and similar to our previous study, no significant differences were detected upon comparing the LIs from all stimulation conditions with the sham condition.

4.2. Behavioral results of the stimulation conditions

Our sham condition results align with the previous DL outcomes, where REA was consistently observed in right-handed populations [51,61,98,99]. Our participants exhibited an average LI of 37.3 ± 24.1, which can be explained by the callosal relay model [40], complemented by the attention-executive model [41]. Since information from the right ear has direct access to the left dominant hemisphere, this provides a built-in advantage for the right ear. In our study, we attempted to manipulate interhemispheric connectivity and LIs by tACS with four different phase lags between the temporal cortices. However, the stimulation conditions did not significantly change the LIs, similar to previous dual-site tACS studies from our research group and others [32,52]. Conversely, an earlier study from the same researchers reported disruptive effects of in-phase gamma and anti-phase delta tACS on interhemispheric integration [29]. This variability suggests that the external phase lag alone cannot fully account for behavioral changes, where interhemispheric connectivity may not be modulated in a one-size-fits-all manner. This complexity in the interaction between stimulation parameters and endogenous connectivity has also been observed in electric field modelling [53].

4.3. Phase lags as a predictive factor

In our current study, we aimed to disentangle this complexity by computing the endogenous phase lags between the target regions and explaining their interactions with the external phase lags. Unlike other forms of NIBS, tACS can uniquely interact with EEG- and MEG-measured brain oscillations in a frequency- and phase-dependent manner [1–3,6,100]. Therefore, it is beneficial to approach this complexity through EEG-based connectivity parameters, specifically focusing on frequency and phase lags between the target regions. To achieve this, we calculated the endogenous 40-Hz phase lags, which could be relevant for the DL task [46,48,49,51]. Since the callosal relay model postulates enhanced interhemispheric connectivity during LE, particularly in terms of enhanced gamma-lagged phase synchrony [40,41,49], these endogenous phase lags in the gamma range should be distinctive between LE and RE, suggesting a possible causal link. Our novel findings revealed a time window between 84 and 112 ms after stimulus presentation, during which these endogenous 40-Hz phase lags differed significantly between LE and RE (Finding 1). This time window should be reproducible over time and imply stable, meaningful results for the gamma range (40 Hz in our case). According to our test-retest reliability results, we successfully demonstrated the reproducibility and stability of the calculated phase lags (Finding 2). Interestingly, this time window encompasses at least one wavelet of 40 Hz in both the main experiment and the test-retest reliability experiment (Finding 3). Additionally, these time windows exhibited on average positive phase lags during left ear reports, indicating a relatively small phase lag, compared to the negative phase lag during right ear reports (finding 4). A similar pattern was detected

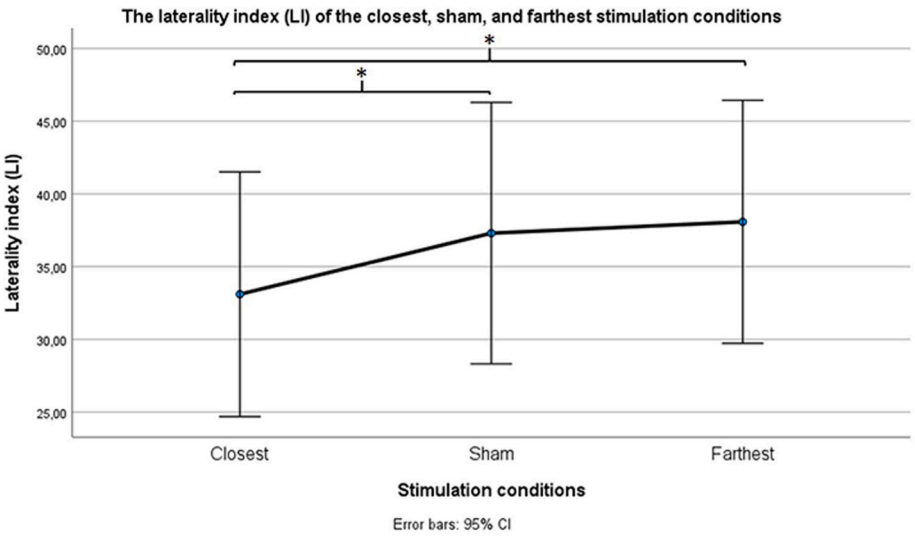

Fig. 5. The endogenous phase lags could explain the changes in LIs. The figure shows the comparison between the closest, sham, and farthest stimulation conditions in terms of the laterality index (LI). The closest and farthest stimulation conditions were defined according to the individual endogenous phase lag for each participant. Using a one-way repeated-measures ANOVA, the comparison of LIs between the closest, sham, and farthest stimulation conditions showed statistical significance ($df = 2$, $F = 3.724$, $p = 0.030$, $\eta^2p = 0.114$). For the post-hoc pairwise comparisons, one-sided paired-sample t-tests revealed statistically lower LI (indicating lower REA) during the closest stimulation condition compared with the sham condition ($t = -2.031$, $df = 29$, $p = 0.026$, BH-corrected $p = 0.039$) and the farthest stimulation condition ($t = -2.449$, $df = 29$, $p = 0.010$, BH-corrected $p = 0.03$). The comparison between the sham and farthest stimulation conditions did not reach significance ($t = -0.440$, $df = 29$, $p = 0.332$, BH-corrected $p = 0.332$). The dots represent the means while the error bars represent the confidence intervals. The asterisk indicates statistical significance ($p < 0.05$).

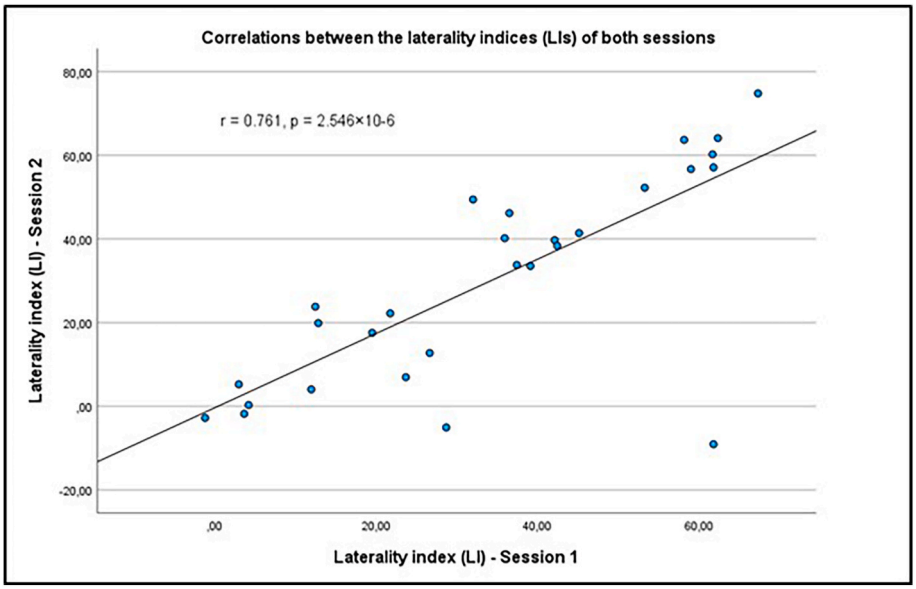

Fig. 6. Correlation between the laterality indices (LIs) of both sessions. The figure shows a scatter plot of the two sessions in terms of LI. Using a Pearson's correlation, the LIs of both sessions are significantly correlated with each other ($r = 0.761$, $p = 2.546 \times 10^{-6}$).

across both sessions of the test-retest reliability. This suggests that the transfer of information from the right to the left side exhibited a significantly smaller phase lag (shorter time difference) during left ear reports compared to right ear reports. This is consistent with the need for faster information transfer between hemispheres for left ear reports to counteract the inherent right ear advantage. Conversely, right ear reports do not necessarily require right-to-left information transfer. Based on Findings 1, 2, 3, and 4, we can infer that these calculated endogenous phase lags may help to predict and explain the heterogeneity of tACS effects on behavioral parameters (LIs).

Having calculated the candidate endogenous phase lags, we correlated them circularly with the LI changes. This analysis revealed a significant correlation only with the LIs from the anti-phasic stimulation (180°) (Fig. 4 Panel (C)), which could be attributed to the circular distribution of our sample (Fig. 4 Panel (B)). Given that many participants exhibited an endogenous phase lag between −45° (315°) and 90°, a substantial number may have experienced a shift towards REA during 180° tACS (indicating a disruptive tACS effect). Additionally, we aimed to personalize our analysis, we defined an optimal and a disruptive stimulation condition for each participant, which could either enhance or disrupt interhemispheric connectivity based on their endogenous phase lags. Our results showed a significant reduction in LI (suggesting enhanced interhemispheric connectivity) during the closest (optimal) stimulation condition compared with both the sham and the farthest

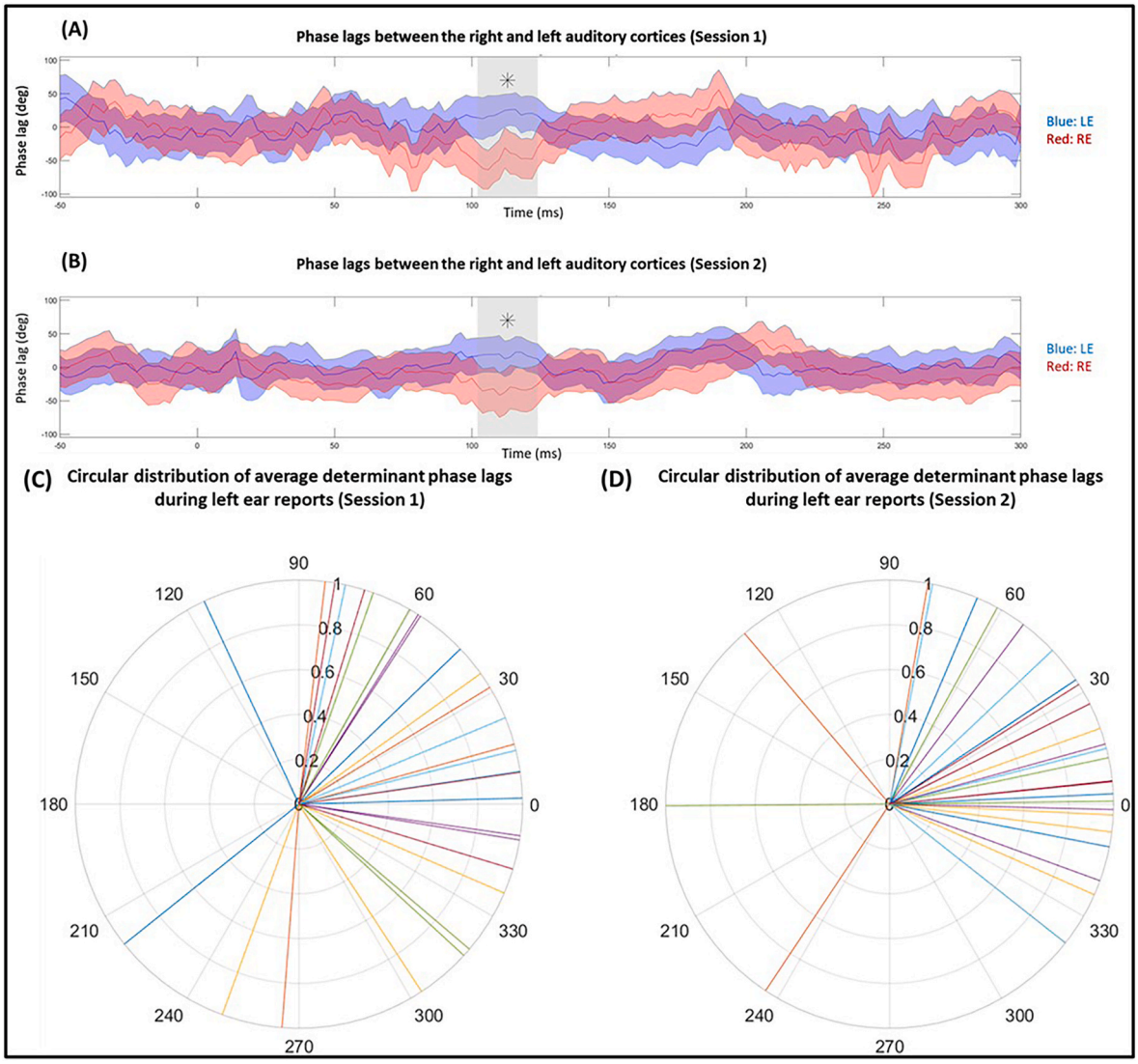

Fig. 7. The time course of phase lags between the right and left secondary auditory cortices Brodmann areas (BAs) 42 and the circular distributions of the endogenous phase lags in both sessions. Panel (A) and (B) show the time course of phase lags for session 1 and session 2, respectively. Compared with RE (in red), LE (in blue) had significantly different phase lags at the time window between 150 and 163 during session 1, which indicates the time window between 100 and 126 ms after the stimulus presentation (p values are shown in S2.2). Session 2 showed an overlapping significant time window between the time points between 151 and 163, i.e., the time window between 102 and 126 ms after the stimulus presentation, except for a near-significance time window 157–158 ($p = 0.069$, other p values are shown in the Supplementary Material S1). The think red and blue lines represent the means, while the shaded areas show the standard deviations. The grey-shaded area with the asterisk indicates the significant time window. The panels (C) and (D) demonstrate circular distributions of the individual endogenous phase lags (average of phase lags within the significant time points during left ear reports (LE) for each participant) within session 1 and session 2, respectively. A significant circular correlation between these phase lags was shown using the statistical test with the function circ_corrcc() provided by the CircStat toolbox ($r = 0.3917$, $p = 0.0224$).

(disruptive) conditions at the individual level. Conversely, the farthest stimulation condition did not statistically increase the LI compared to the sham.

4.4. Phase lags in previous dual-site tACS studies

Dual-site tACS has been extensively applied in previous studies to modulate interregional connectivity in the brain during various cognitive tasks, utilizing different stimulation frequencies. However, there is no consensus regarding the optimal stimulation phase lags. Some studies detected behavioral effects with in-phase [13–15,17,18,23–29] or anti-phase [14,16,19,21,28–30,101] stimulations, while others did not report any effects at all [31]. Interestingly, some in-phase experiments altered inter-regional connectivity as measured by EEG [13–15,18,24,25,28], or fMRI [17], while anti-phase protocols using EEG [16,21,28,30,101], or fMRI [52,53] have also shown connectivity effects. Notably, some of these publications report effects on interhemispheric communication [13,15,16,52,53]. In other words, we report similar effects to the non-uniformity observed in DL results [29,32,52]. This variability suggests the absence of a one-size-fits-all protocol for coupling or decoupling two brain regions, highlighting the need for further optimization of stimulation parameters. In this context, four main optimization aspects should be considered based on these previous studies.

First, the connectivity between the two candidate regions may be direct or indirect (i.e., the nature of communication). In the case of a direct causal connection (i.e., one region drives the activity in the other), a nonzero-phase lag might be optimal, as the naturalistic connection would necessitate such a phase relationship [22,89]. Conversely, if a tertiary hub modulates the functional connectivity between the two brain regions, in-phase (zero-phase lag) stimulation could potentially

enhance their coupling, as has been effectively simulated [13,22,28]. In our case of DL, both BAs 42 are directly and causally connected to ensure interhemispheric connectivity, particularly during LE [102], which might explain the lack of response to in-phase stimulation (0°).

Second, the enhancing effects of bifocal-tACS may be easier to achieve than its disruptive effects. This might explain why some studies have only demonstrated enhancement of EEG-based interregional connectivity via tACS with a certain phase lag, without being able to disrupt connectivity with an opposite phase lag [24]. In this context, it might be harder for the opposite phase lag to generate the expected results due to the timing dependency of both entrainment and synaptic changes. Our results exhibited a similar pattern, where the farthest stimulation condition based on EEG-extracted phase lags did not achieve the expected behavioral outcome (enhanced REA). Conversely, previous work on dichotic listening demonstrated disruptive effects of anti-phase stimulation on interhemispheric connectivity, although these effects were measured using fMRI [52].

Third, some tACS-induced changes may be either entrainment- or plasticity-dependent, which would manifest as either online or offline effects, respectively [18,21,24,25,27], and can be simulated with network models [103]. In our case, the connectivity between BAs 42 during LE was likely entrainment-dependent, but future studies could investigate the aftereffects of bifocal-tACS to uncover its neuroplastic role.

Fourth, the baseline endogenous phase lag between target brain regions could predict the effects of tACS at different phase lags, especially since previous studies have suggested that tACS effects depend on internal brain states, including individual endogenous phase lags, cross-frequency coupling, inherent wave propagation speeds, and the level of cognitive demands [17,18,26,30,32]. In our DL study, the endogenous phase lags were able to explain the behavioral changes during tACS, with the closest stimulation condition enhancing the left ear reports. These four optimization aspects warrant further investigation in future research.

4.5. Limitations of the current study

Although we managed to suggest the predictive effects of the endogenous phase lags during bi-temporal tACS, our study still has some significant limitations. First, the limited spatial resolution of the LORETA software poses a major localization issue. However, we tried to overcome this by focusing on centroid voxels within BAs 42. Additionally, previous studies have somewhat validated eLORETA localization using simultaneous EEG and fMRI [104,105]. Second, we applied pre-set stimulation protocols with fixed parameters, notably the phase lags and the frequency, without personalization. Future studies could aim to apply a more personalized approach, considering the closest and farthest phase lags and the individual peak frequencies. Third, although the electrode placement was validated via the ROAST software, it could be further individualized using structural imaging techniques [106]. Fourth, we recruited only males for the test-retest reliability, and both females and males for the main experiment. Therefore, we cannot completely exclude the effects of the different menstrual phases on the gamma oscillations. Fifth, the current study did not take into consideration the phase relationship between the tACS current and the presented sound stimuli [29,52,107–110]. Future research could try to address this issue with closed-loop tACS.

5. Conclusions

In this study, we investigated the effects of bitemporal 40-Hz tACS with four different phase lags (0°, 45°, 90°, and 180°) during a dichotic listening task (DL) behavioral perception, in comparison with a sham condition. Our findings reveal, for the first time, that the interaction between endogenous and external phase lags is a predictive factor for bifocal-tACS effects at the individual level. Consistent with our hypothesis, endogenous phase lags allowed us to identify both optimal and disruptive stimulation conditions for each participant. Specifically, the stimulation condition closest to the endogenous phase lag (optimal) led to a significant reduction in the LI, indicating enhanced interhemispheric connectivity compared to both the sham and the farthest (disruptive) conditions. Conversely, the farthest stimulation condition did not statistically increase the LI relative to the sham condition. These findings underscore the importance of considering endogenous phase lags and their interaction with external tACS phase lags in dual-site tACS studies. Future research should explore three additional factors: the nature of communication between target regions (direct vs. indirect), the differential effects of tACS (enhancing vs. disruptive), and the underlying mechanisms of action (entrainment vs. neuroplasticity). In summary, our finding of a significant interaction between endogenous and external phase lags suggests a novel approach for achieving more consistent and targeted bifocal-tACS effects on interregional connectivity.

CRediT authorship contribution statement

Osama Elyamany: Writing – review & editing, Writing – original draft, Visualization, Validation, Software, Methodology, Investigation, Formal analysis. **Jona Iffland:** Writing – review & editing, Writing – original draft, Visualization, Validation, Software, Methodology, Investigation, Formal analysis. **Josef Bak:** Writing – review & editing, Software, Methodology, Investigation. **Cornelius Classen:** Writing – review & editing, Validation, Investigation. **Guido Nolte:** Writing – review & editing, Software, Formal analysis. **Till R. Schneider:** Writing – review & editing, Software, Formal analysis. **Gregor Leicht:** Writing – review & editing, Supervision, Methodology, Funding acquisition, Conceptualization. **Christoph Mulert:** Writing – review & editing, Writing – original draft, Validation, Supervision, Methodology, Funding acquisition, Formal analysis, Conceptualization.

Data availability

Requests for further information and resources should be directed to and will be fulfilled by the corresponding author, Osama Elyamany (osama.elyamany@psychiat.med.uni-giessen.de).

Compliance with ethical standards

This work included the recruitment of human participants at the research lab of the Department of Psychiatry at Justus Liebig University Giessen in Germany after signing an informed consent. The whole work was carried out according to the approval of the ethical committee at the Faculty of Medicine (FB 11 Medizin), Justus-Liebig University Giessen, registered with the project number “AZ 34/19”.

Declaration of generative AI and AI-assisted technologies in the writing process

During the preparation of this work, the authors used ChatGPT in order to correct spelling and grammatical errors and enhance the readability of the manuscript. After using this tool, the authors reviewed and edited the content as needed and take full responsibility for the content of the publication.

Declaration of competing interest

The authors declare that they have no known competing financial interests or personal relationships that could have appeared to influence the work reported in this paper.

Acknowledgements

This work was funded by:(1) the German Research Foundation (DFG: www.dfg.de) through two projects: (a) the Collaborative Research Centre SFB936-Project C6-Third Funding Period to C. Mulert and G. Leicht, and (b) the Collaborative Research Centre SFB/TRR135-Project B7-Third Funding Period to C. Mulert; and (2) the DYNAMIC Centre, funded by the LOEWE program of the Hessian Ministry of Science and Arts (Grant Number: LOEWE 1/16/519/03/09.001 (0009)/98).

Appendix A. Supplementary data

Supplementary data to this article can be found online at https://doi.org/10.1016/j.brs.2025.04.011.

Glossary

ANOVA	Analysis of variance
BAs	Brodmann areas
BH	Benjamini-Hochberg
CV	Consonant-vowel
dB	Decibel
DL:	Dichotic Listening
EEG	Electroencephalography
EHI	Edinburgh Handedness Inventory
eLORETA	Exact low-resolution brain electromagnetic tomography
EOG	Electrooculography
fMRI	Functional magnetic resonance imaging
HEOGL:	Left horizontal Electrooculography
HEOGR	Right horizontal Electrooculography
Hz	Hertz
LE	Left ear reports
LI	Laterality index
ms	Millisecond
NIBS	Non-invasive brain stimulation
RE	Right ear reports
REA	Right-ear advantage
REOG	Radial electrooculography
ROIs	Regions of interest
SD	Standard deviation
tACS	Transcranial alternating current stimulation
VEOGI	Inferior vertical electrode
VEOGS	Superior vertical electrode

References

[1] Liu A, Vöröslakos M, Kronberg G, Henin S, Krause MR, Huang Y, et al. Immediate neurophysiological effects of transcranial electrical stimulation. Nat Commun 2018;9(1):5092. https://doi.org/10.1038/s41467-018-07233-7.
[2] Deans JK, Powell AD, Jefferys JGR. Sensitivity of coherent oscillations in rat hippocampus to AC electric fields. J Physiol 2007;583(Pt 2):555–65. https://doi.org/10.1113/jphysiol.2007.137711.
[3] Ali MM, Sellers KK, Fröhlich F. Transcranial alternating current stimulation modulates large-scale cortical network activity by network resonance. J Neurosci 2013;33(27):11262–75. https://doi.org/10.1523/JNEUROSCI.5867-12.2013.
[4] Fehér KD, Nakataki M, Morishima Y. Phase-dependent modulation of signal transmission in cortical networks through tACS-induced neural oscillations. Front Hum Neurosci 2017;11:471. https://doi.org/10.3389/fnhum.2017.00471.
[5] Riecke L, Formisano E, Herrmann CS, Sack AT. 4-Hz transcranial alternating current stimulation phase modulates hearing. Brain Stimul 2015;8(4):777–83. https://doi.org/10.1016/j.brs.2015.04.004.
[6] Elyamany O, Leicht G, Herrmann CS, Mulert C. Transcranial alternating current stimulation (tACS): from basic mechanisms towards first applications in psychiatry. Eur Arch Psychiatr Clin Neurosci 2021;271(1):135–56. https://doi.org/10.1007/s00406-020-01209-9.
[7] Hopfinger JB, Parsons J, Fröhlich F. Differential effects of 10-Hz and 40-Hz transcranial alternating current stimulation (tACS) on endogenous versus exogenous attention. Cognit Neurosci 2017;8(2):102–11. https://doi.org/10.1080/17588928.2016.1194261.
[8] Chai Y, Sheng J, Bandettini PA, Gao J-H. Frequency-dependent tACS modulation of BOLD signal during rhythmic visual stimulation. Hum Brain Mapp 2018;39(5):2111–20. https://doi.org/10.1002/hbm.23990.
[9] Gaugain G, Al Harrach M, Yochum M, Wendling F, Bikson M, Modolo J, et al. Frequency-dependent phase entrainment of cortical cell types during tACS: converging modeling evidence. 2023.
[10] Antal A, Herrmann CS. Transcranial alternating current and random noise stimulation: possible mechanisms. Neural Plast 2016;2016:3616807. https://doi.org/10.1155/2016/3616807.
[11] Krause MR, Vieira PG, Csorba BA, Pilly PK, Pack CC. Transcranial alternating current stimulation entrains single-neuron activity in the primate brain. Proc Natl Acad Sci U S A 2019;116(12):5747–55. https://doi.org/10.1073/pnas.1815958116.
[12] Reato D, Rahman A, Bikson M, Parra LC. Low-intensity electrical stimulation affects network dynamics by modulating population rate and spike timing. J Neurosci 2010;30(45):15067–79. https://doi.org/10.1523/JNEUROSCI.2059-10.2010.
[13] Schwab BC, Misselhorn J, Engel AK. Modulation of large-scale cortical coupling by transcranial alternating current stimulation. Brain Stimul 2019;12(5):1187–96. https://doi.org/10.1016/j.brs.2019.04.013.
[14] Reinhart RMG, Nguyen JA. Working memory revived in older adults by synchronizing rhythmic brain circuits. Nat Neurosci 2019;22(5):820–7. https://doi.org/10.1038/s41593-019-0371-x.
[15] Helfrich RF, Knepper H, Nolte G, Strüber D, Rach S, Herrmann CS, et al. Selective modulation of interhemispheric functional connectivity by HD-tACS shapes perception. PLoS Biol 2014;12(12):e1002031. https://doi.org/10.1371/journal.pbio.1002031.
[16] Strüber D, Rach S, Trautmann-Lengsfeld SA, Engel AK, Herrmann CS. Antiphasic 40 Hz oscillatory current stimulation affects bistable motion perception. Brain Topogr 2014;27(1):158–71. https://doi.org/10.1007/s10548-013-0294-x.
[17] Violante IR, Li LM, Carmichael DW, Lorenz R, Leech R, Hampshire A, et al. Externally induced frontoparietal synchronization modulates network dynamics and enhances working memory performance. Elife 2017;6. https://doi.org/10.7554/eLife.22001.
[18] Meng Q, Zhu Y, Yuan Y, Ni R, Yang L, Liu J, et al. Dual-site beta tACS over rIFG and M1 enhances response inhibition: a parallel multiple control and replication study. Int J Clin Health Psychol 2023;23(4):100411. https://doi.org/10.1016/j.ijchp.2023.100411.
[19] Yaple Z, Vakhrushev R. Modulation of the frontal-parietal network by low intensity anti-phase 20 Hz transcranial electrical stimulation boosts performance in the attentional blink task. Int J Psychophysiol 2018;127:11–6. https://doi.org/10.1016/j.ijpsycho.2018.02.014.
[20] Polanía R, Moisa M, Opitz A, Grueschow M, Ruff CC. The precision of value-based choices depends causally on fronto-parietal phase coupling. Nat Commun 2015;6(1):8090. https://doi.org/10.1038/ncomms9090.
[21] Zhang L, Chen L, Wang Z, Liu X, Ming D. Enhancing motor imagery performance by antiphasic 10 Hz transcranial alternating current stimulation. IEEE Trans Neural Syst Rehabil Eng 2023;31:2747–57. https://doi.org/10.1109/TNSRE.2023.3286419.
[22] Saturnino GB, Madsen KH, Siebner HR, Thielscher A. How to target inter-regional phase synchronization with dual-site Transcranial Alternating Current Stimulation. Neuroimage 2017;163:68–80. https://doi.org/10.1016/j.neuroimage.2017.09.024.
[23] Polanía R, Nitsche MA, Korman C, Batsikadze G, Paulus W. The importance of timing in segregated theta phase-coupling for cognitive performance. Curr Biol 2012;22(14):1314–8. https://doi.org/10.1016/j.cub.2012.05.021.
[24] Hu Z, Samuel IBH, Meyyappan S, Bo K, Rana C, Ding M. Aftereffects of frontoparietal theta tACS on verbal working memory: behavioral and neurophysiological analysis. IBRO Neurosci. Rep. 2022;13:469–77. https://doi.org/10.1016/j.ibneur.2022.10.013.
[25] Fujiyama H, Williams A, Tan J, Levin O, Hinder MR. Comparison of online and offline applications of dual-site transcranial alternating current stimulation (tACS) over the pre-supplementary motor area (preSMA) and right inferior frontal gyrus (rIFG) for improving response inhibition. Neuropsychologia 2023;191:108737. https://doi.org/10.1016/j.neuropsychologia.2023.108737.
[26] Draaisma LR, Wessel MJ, Moyne M, Morishita T, Hummel FC. Targeting the frontoparietal network using bifocal transcranial alternating current stimulation during a motor sequence learning task in healthy older adults. Brain Stimul 2022;15(4):968–79. https://doi.org/10.1016/j.brs.2022.06.012.
[27] Heise K-F, Monteiro TS, Leunissen I, Mantini D, Swinnen SP. Distinct online and offline effects of alpha and beta transcranial alternating current stimulation (tACS) on continuous bimanual performance and task-set switching. Sci Rep 2019;9(1):3144. https://doi.org/10.1038/s41598-019-39900-0.
[28] Reinhart RMG. Disruption and rescue of interareal theta phase coupling and adaptive behavior. Proc Natl Acad Sci U S A 2017;114(43):11542–7. https://doi.org/10.1073/pnas.1710257114.
[29] Preisig BC, Sjerps MJ, Hervais-Adelman A, Kösem A, Hagoort P, Riecke L. Bilateral gamma/delta transcranial alternating current stimulation affects interhemispheric speech sound integration. J Cognit Neurosci 2020;32(7):1242–50. https://doi.org/10.1162/jocn_a_01498.
[30] Salamanca-Giron RF, Raffin E, Zandvliet SB, Seeber M, Michel CM, Sauseng P, et al. Enhancing visual motion discrimination by desynchronizing bifocal oscillatory activity. Neuroimage 2021;240:118299. https://doi.org/10.1016/j.neuroimage.2021.118299.
[31] Preisig BC, Sjerps MJ, Kösem A, Riecke L. Dual-site high-density 4Hz transcranial alternating current stimulation applied over auditory and motor cortical speech areas does not influence auditory-motor mapping. Brain Stimul 2019;12(3):775–7. https://doi.org/10.1016/j.brs.2019.01.007.

[32] Meier J, Nolte G, Schneider TR, Engel AK, Leicht G, Mulert C. Intrinsic 40Hz-phase asymmetries predict tACS effects during conscious auditory perception. PLoS One 2019;14(4):e0213996. https://doi.org/10.1371/journal.pone.0213996.
[33] Frohlich F, Townsend L. Closed-loop transcranial alternating current stimulation: towards personalized non-invasive brain stimulation for the treatment of psychiatric illnesses. Curr Behav Neurosci Rep 2021;8(2):51–7. https://doi.org/10.1007/s40473-021-00227-8.
[34] Kinsbourne M. The cerebral basis of lateral asymmetries in attention. Acta Psychol 1970;33:193–201. https://doi.org/10.1016/0001-6918(70)90132-0.
[35] Cheatham BH. Speech and music draw attention to the right ear in stereophonic listening. PMS 1990;70(1):227. https://doi.org/10.2466/PMS.70.1.227-231.
[36] Hiscock M, Kinsbourne M. Attention and the right-ear advantage: what is the connection? Brain Cognit 2011;76(2):263–75. https://doi.org/10.1016/j.bandc.2011.03.016.
[37] Kimura D. Some effects of temporal-lobe damage on auditory perception. Canadian J. Psychol. Revue canadienne de psychologie 1961;15(3):156–65. https://doi.org/10.1037/h0083218.
[38] Kimura D. Cerebral dominance and the perception of verbal stimuli. Canadian J. Psychol. Revue canadienne de psychologie 1961;15(3):166–71. https://doi.org/10.1037/h0083219.
[39] Pollmann S, Maertens M, Cramon DY von, Lepsien J, Hugdahl K. Dichotic listening in patients with splenial and nonsplenial callosal lesions. Neuropsychology 2002;16(1):56–64. https://doi.org/10.1037//0894-4105.16.1.56.
[40] Zaidel E. Disconnection syndrome as a model for laterality effects in the normal brain. In: Hellige JB, Hellige JB, editors. Cerebral hemisphere asymmetry. New York: Praeger; 1983.
[41] Hugdahl K, Westerhausen R. Speech processing asymmetry revealed by dichotic listening and functional brain imaging. Neuropsychologia 2016;93(Pt B):466–81. https://doi.org/10.1016/j.neuropsychologia.2015.12.011.
[42] Brancucci A, Babiloni C, Babiloni F, Galderisi S, Mucci A, Tecchio F, et al. Inhibition of auditory cortical responses to ipsilateral stimuli during dichotic listening: evidence from magnetoencephalography. Eur J Neurosci 2004;19(8):2329–36. https://doi.org/10.1111/j.0953-816X.2004.03302.x.
[43] Momtaz S, Moncrieff D, Bidelman GM. Dichotic listening deficits in amblyaudia are characterized by aberrant neural oscillations in auditory cortex. Clin Neurophysiol: off. J. Int. Fed. Clin. Neurophysiol 2021;132(9):2152–62. https://doi.org/10.1016/j.clinph.2021.04.022.
[44] Razumnikova OM, Vol'f NV. Gender differences in interhemisphere interactions during distributed and directed attention. Neurosci Behav Physiol 2007;37(5):429–34. https://doi.org/10.1007/s11055-007-0031-6.
[45] Solcà M, Mottaz A, Guggisberg AG. Binaural beats increase interhemispheric alpha-band coherence between auditory cortices. Hear Res 2016;332:233–7. https://doi.org/10.1016/j.heares.2015.09.011.
[46] Steinmann S, Amselberg R, Cheng B, Thomalla G, Engel AK, Leicht G, et al. The role of functional and structural interhemispheric auditory connectivity for language lateralization - a combined EEG and DTI study. Sci Rep 2018;8(1):15428. https://doi.org/10.1038/s41598-018-33586-6.
[47] Steinmann S, Leicht G, Andreou C, Polomac N, Mulert C. Auditory verbal hallucinations related to altered long-range synchrony of gamma-band oscillations. Sci Rep 2017;7(1):8401. https://doi.org/10.1038/s41598-017-09253-7.
[48] Steinmann S, Leicht G, Ertl M, Andreou C, Polomac N, Westerhausen R, et al. Conscious auditory perception related to long-range synchrony of gamma oscillations. Neuroimage 2014;100:435–43. https://doi.org/10.1016/j.neuroimage.2014.06.012.
[49] Steinmann S, Meier J, Nolte G, Engel AK, Leicht G, Mulert C. The callosal relay model of interhemispheric communication: new evidence from effective connectivity analysis. Brain Topogr 2018;31(2):218–26. https://doi.org/10.1007/s10548-017-0583-x.
[50] Thiebes S, Steinmann S, Curic S, Polomac N, Andreou C, Eichler I-C, et al. Alterations in interhemispheric gamma-band connectivity are related to the emergence of auditory verbal hallucinations in healthy subjects during NMDA-receptor blockade. Neuropsychopharmacology 2018;43(7):1608–15. https://doi.org/10.1038/s41386-018-0014-z.
[51] Elyamany O, Iffland J, Lockhofen D, Steinmann S, Leicht G, Mulert C. Top-down modulation of dichotic listening affects interhemispheric connectivity: an electroencephalography study. Front Neurosci 2024;18. https://doi.org/10.3389/fnins.2024.1424746.
[52] Preisig BC, Riecke L, Sjerps MJ, Kösem A, Kop BR, Bramson B, et al. Selective modulation of interhemispheric connectivity by transcranial alternating current stimulation influences binaural integration. Proc Natl Acad Sci U S A 2021;118(7). https://doi.org/10.1073/pnas.2015488118.
[53] Preisig BC, Hervais-Adelman A. The predictive value of individual electric field modeling for transcranial alternating current stimulation induced brain modulation. Front Cell Neurosci 2022;16:818703. https://doi.org/10.3389/fncel.2022.818703.
[54] Raine A. The SPQ: a scale for the assessment of schizotypal personality based on DSM-III-R criteria. Schizophr Bull 1991;17(4):555–64. https://doi.org/10.1093/schbul/17.4.555.
[55] Oldfield RC. The assessment and analysis of handedness: the Edinburgh inventory. Neuropsychologia 1971;9(1):97–113. https://doi.org/10.1016/0028-3932(71)90067-4.
[56] Voglmaier MM, Seidman LJ, Niznikiewicz MA, Madan A, Dickey CC, Shenton ME, et al. Dichotic listening in schizotypal personality disorder: evidence for gender and laterality effects. Schizophr Res 2009;115(2–3):290–2. https://doi.org/10.1016/j.schres.2009.04.028.
[57] Antal A, Alekseichuk I, Bikson M, Brockmöller J, Brunoni AR, Chen R, et al. Low intensity transcranial electric stimulation: safety, ethical, legal regulatory and application guidelines. Clin Neurophysiol 2017;128(9):1774–809. https://doi.org/10.1016/j.clinph.2017.06.001.
[58] Matsumoto H, Ugawa Y. Adverse events of tDCS and tACS: a review. Clinical Neurophysiology Practice 2017;2:19–25. https://doi.org/10.1016/j.cnp.2016.12.003.
[59] Woods AJ, Antal A, Bikson M, Boggio PS, Brunoni AR, Celnik P, et al. A technical guide to tDCS, and related non-invasive brain stimulation tools. Clin Neurophysiol 2016;127(2):1031–48. https://doi.org/10.1016/j.clinph.2015.11.012.
[60] Esser Audio Software. Home Audiometer Hearing Test. [February 03, 2023]; Available from: http://www.esseraudio.com/index.php/en/home-audiometer-hearing-test.
[61] Westerhausen R, Kompus K. How to get a left-ear advantage: a technical review of assessing brain asymmetry with dichotic listening. Scand J Psychol 2018;59(1):66–73. https://doi.org/10.1111/sjop.12408.
[62] Neurobehavioral Systems. [February 03, 2023]; Available from: https://www.neurobs.com/.
[63] neuroConn: DC-STIMULATOR MC | neurocare technology. Available from, https://www.neurocaregroup.com/technology/dc-stimulator-mc. [Accessed 13 June 2024].
[64] Huang Y, Datta A, Bikson M, Parra LC. Realistic volumetric-approach to simulate transcranial electric stimulation-ROAST-a fully automated open-source pipeline. J Neural Eng 2019;16(5):56006. https://doi.org/10.1088/1741-2552/ab208d.
[65] Karnath HO. New insights into the functions of the superior temporal cortex. Nat Rev Neurosci 2001;2(8):568–76. https://doi.org/10.1038/35086057.
[66] Chauhan P, Rathawa A, Jethwa K, Mehra S. Cerebral ischemia: the anatomy of the cerebral cortex, vol. 1; 2021. p. 1–16. https://doi.org/10.36255/exonpublications.cerebralischemia.2021.cerebralcortex.
[67] EASYCAP. Easycap EEG touch-proof Ag/AgCl electrodes. Available from: https://shop.easycap.de/collections/electrodes; June 13, 2024.
[68] ParkerLabs. Signagel® electrode gel - ParkerLabs. [June 13, 2024].
[69] Brain Products GmbH. BrainAmp series | brain products GmbH > solutions. Available from: https://www.brainproducts.com/solutions/brainamp/; [June 13, 2024.
[70] EASYCAP. Abralyt 2000. [June 13, 2024]; Available from: https://shop.easycap.de/products/abralyt-2000.
[71] Brain Products GmbH. Download BrainVision Recorder | Brain Products GmbH. [June 13, 2024]; Available from: https://www.brainproducts.com/downloads/recorder/.
[72] Brain Products GmbH. Download BrainVision Analyzer | Brain Products GmbH. [June 13, 2024]; Available from: https://www.brainproducts.com/downloads/analyzer/.
[73] Keren AS, Yuval-Greenberg S, Deouell LY. Saccadic spike potentials in gamma-band EEG: characterization, detection and suppression. Neuroimage 2010;49(3):2248–63. https://doi.org/10.1016/j.neuroimage.2009.10.057.
[74] Klug M, Gramann K. Identifying key factors for improving ICA-based decomposition of EEG data in mobile and stationary experiments. Eur J Neurosci 2021;54(12):8406–20. https://doi.org/10.1111/ejn.14992.
[75] Delorme A, Makeig S. EEGLAB: an open source toolbox for analysis of single-trial EEG dynamics including independent component analysis. J Neurosci Methods 2004;134(1):9–21. https://doi.org/10.1016/j.jneumeth.2003.10.009.
[76] Widmann A, Schröger E, Maess B. Digital filter design for electrophysiological data–a practical approach. J Neurosci Methods 2015;250:34–46. https://doi.org/10.1016/j.jneumeth.2014.08.002.
[77] Mullen T. CleanLine EEGLAB plugin. Neuroimaging informatics tools and resources clearinghouse (NITRC). 2012. San Diego, CA.
[78] eLORETA. LOW RESOLUTION BRAIN ELECTROMAGNETIC TOMOGRAPHY, LORETA, sLORETA, eLORETA, by R.D. Pascual-Marqui. [October 21, 2021]; Available from: http://www.uzh.ch/keyinst/loreta.htm.
[79] Pascual-Marqui RD. Instantaneous and lagged measurements of linear and nonlinear dependence between groups of multivariate time series: frequency decomposition. 2007.
[80] Pascual-Marqui RD, Lehmann D, Koukkou M, Kochi K, Anderer P, Saletu B, et al. Assessing interactions in the brain with exact low-resolution electromagnetic tomography. Phil. Trans. R. Soc. A. 2011;369:3768–84. https://doi.org/10.1098/rsta.2011.0081. 1952.
[81] Lancaster JL, Woldorff MG, Parsons LM, Liotti M, Freitas CS, Rainey L, et al. Automated Talairach Atlas labels for functional brain mapping. Hum Brain Mapp 2000;10(3):120–31. https://doi.org/10.1002/1097-0193(200007)10:3<120:aid-hbm30>3.0.co. 2-131.
[82] Python.org. Welcome to Python.org. [October 21, 2021]; Available from: https://www.python.org/.
[83] MATLAB. version 9.12 (R2022a). Natick, Massachusetts: The MathWorks Inc; 2022.
[84] Nolte G, Galindo-Leon E, Li Z, Liu X, Engel AK. Mathematical relations between measures of brain connectivity estimated from electrophysiological recordings for Gaussian distributed data. Front Neurosci 2020;14:577574. https://doi.org/10.3389/fnins.2020.577574.
[85] Stam CJ, Nolte G, Daffertshofer A. Phase lag index: assessment of functional connectivity from multi channel EEG and MEG with diminished bias from common sources. Hum Brain Mapp 2007;28(11):1178–93. https://doi.org/10.1002/hbm.20346.

[86] Lachaux J-P, Rodriguez E, Martinerie J, Varela FJ. Measuring phase synchrony in brain signals. Hum Brain Mapp 1999;8(4):194–208. https://doi.org/10.1002/(SICI)1097-0193(1999)8:4<194:AID-HBM4>3.0.CO;2-C.
[87] Rosenblum MG, Pikovsky AS, Kurths J. Phase synchronization of chaotic oscillators. Phys Rev Lett 1996;76(11):1804–7. https://doi.org/10.1103/PhysRevLett.76.1804.
[88] Berens P. CircStat A MATLAB toolbox for circular statistics. J Stat Software 2009;31(10). https://doi.org/10.18637/jss.v031.i10.
[89] Nolte G, Bai O, Wheaton L, Mari Z, Vorbach S, Hallett M. Identifying true brain interaction from EEG data using the imaginary part of coherency. Clin Neurophysiol 2004;115(10):2292–307. https://doi.org/10.1016/j.clinph.2004.04.029.
[90] Haraguchi R, Hoshi H, Ichikawa S, Hanyu M, Nakamura K, Fukasawa K, et al. The menstrual cycle alters resting-state cortical activity: a magnetoencephalography study. Front Hum Neurosci 2021;15:652789. https://doi.org/10.3389/fnhum.2021.652789.
[91] Sumner RL, McMillan RL, Shaw AD, Singh KD, Sundram F, Muthukumaraswamy SD. Peak visual gamma frequency is modified across the healthy menstrual cycle. Hum Brain Mapp 2018;39(8):3187–202. https://doi.org/10.1002/hbm.24069.
[92] Brain Products GmbH. actiCAP active Electrodes Walkthrough. [August 03, 2024]; Available from: https://pressrelease.brainproducts.com/active-electrodes-walkthrough/.
[93] Blair RC, Karniski W. An alternative method for significance testing of waveform difference potentials. Psychophysiology 1993;30(5):518–24. https://doi.org/10.1111/j.1469-8986.1993.tb02075.x.
[94] Nolte Guido. MEG and EEG toolbox of hamburg (METH). Hamburg: Neurophysiology and Pathophysiology, University Medical Center Hamburg-Eppendorf; 2019.
[95] Benjamini Y, Hochberg Y. Controlling the false discovery rate: a practical and powerful approach to multiple testing. J Roy Stat Soc B Stat Methodol 1995;57(1):289–300. https://doi.org/10.1111/j.2517-6161.1995.tb02031.x.
[96] JASP Team. JASP (version 0.18.3) [Computer software] Available from: https://jasp-stats.org/; 2024.
[97] IBM SPSS statistics for windows. IBM corp. Armonk, NY: IBM Corp; 2022.
[98] Westerhausen R, Bless JJ, Passow S, Kompus K, Hugdahl K. Cognitive control of speech perception across the lifespan: a large-scale cross-sectional dichotic listening study. Dev Psychol 2015;51(6):806–15. https://doi.org/10.1037/dev0000014.
[99] Westerhausen R, Bless J, Kompus K. Behavioral laterality and aging: the free-recall dichotic-listening right-ear advantage increases with age. Dev Neuropsychol 2015;40(5):313–27. https://doi.org/10.1080/87565641.2015.1073291.
[100] Helfrich RF, Schneider TR, Rach S, Trautmann-Lengsfeld SA, Engel AK, Herrmann CS. Entrainment of brain oscillations by transcranial alternating current stimulation. Curr Biol 2014;24(3):333–9. https://doi.org/10.1016/j.cub.2013.12.041.
[101] Alekseichuk I, Pabel SC, Antal A, Paulus W. Intrahemispheric theta rhythm desynchronization impairs working memory. Restor Neurol Neurosci 2017;35(2):147–58. https://doi.org/10.3233/RNN-160714.
[102] Musiek FE, Weihing J. Perspectives on dichotic listening and the corpus callosum. Brain Cognit 2011;76(2):225–32. https://doi.org/10.1016/j.bandc.2011.03.011.
[103] Schwab BC, König P, Engel AK. Spike-timing-dependent plasticity can account for connectivity aftereffects of dual-site transcranial alternating current stimulation. Neuroimage 2021;237:118179. https://doi.org/10.1016/j.neuroimage.2021.118179.
[104] Mulert C, Jäger L, Propp S, Karch S, Störmann S, Pogarell O, et al. Sound level dependence of the primary auditory cortex: simultaneous measurement with 61-channel EEG and fMRI. Neuroimage 2005;28(1):49–58. https://doi.org/10.1016/j.neuroimage.2005.05.041.
[105] Mulert C, Jäger L, Schmitt R, Bussfeld P, Pogarell O, Möller H-J, et al. Integration of fMRI and simultaneous EEG: towards a comprehensive understanding of localization and time-course of brain activity in target detection. Neuroimage 2004;22(1):83–94. https://doi.org/10.1016/j.neuroimage.2003.10.051.
[106] Kasten FH, Duecker K, Maack MC, Meiser A, Herrmann CS. Integrating electric field modeling and neuroimaging to explain inter-individual variability of tACS effects. Nat Commun 2019;10(1):5427. https://doi.org/10.1038/s41467-019-13417-6.
[107] Kösem A, Bosker HR, Jensen O, Hagoort P, Riecke L. Biasing the perception of spoken words with transcranial alternating current stimulation. J Cognit Neurosci 2020;32(8):1428–37. https://doi.org/10.1162/jocn_a_01579.
[108] Riecke L, Formisano E, Sorger B, Başkent D, Gaudrain E. Neural entrainment to speech modulates speech intelligibility. Curr Biol 2018;28(2):161–169.e5. https://doi.org/10.1016/j.cub.2017.11.033.
[109] Wilsch A, Neuling T, Obleser J, Herrmann CS. Transcranial alternating current stimulation with speech envelopes modulates speech comprehension. Neuroimage 2018;172:766–74. https://doi.org/10.1016/j.neuroimage.2018.01.038.
[110] Zoefel B, Archer-Boyd A, Davis MH. Phase entrainment of brain oscillations causally modulates neural responses to intelligible speech. Curr Biol 2018;28(3):401–408.e5. https://doi.org/10.1016/j.cub.2017.11.071.